

Problem No. UDRI-4

Title: Comparative Risk Assessment of the Thinning Effect of Corrosion in a Representative Lap Joint

Objective:

To illustrate the use of PROF for the calculation of the failure probability of a lap joint in the presence of various degrees of corrosive thinning.

General Description:

This sample problem illustrates the use of the PROF risk analysis computer program for evaluating the probability of failure of a lap joint with various degrees of corrosion and two different multi-site damage scenarios. The cracking scenarios are from test specimens but are considered representative of corrosion in lap joints. The analyses requires multiple runs of PROF with each given a different structural condition. The multiple runs are then combined based on the probability of occurrence on the conditions. Inspection intervals based on crack growth in pristine structure are compared with those assuming the presence of corrosion and multi-site damage.

Topics Covered: Failure probability, conditional probabilities, multiple element damage

Type of Structure: Wing chordwise joint, beam cap, splice fitting

Relevant Sections of Handbook: Section 8

Authors: Alan P. Berens and Peter W. Hovey

Company Name: University of Dayton Research Institute
Structural Integrity Division
Dayton, OH 45469-0120
937-229-4417
www.udri.udayton.edu

Contact Point: Alan P. Berens
Phone: 937-229-4475
e-Mail: Berens@udri.udayton.edu



Overview of Problem Description

The example risk analysis of a lap joint with MSD and corrosion is based on data from a specimen that is representative of a fuselage lap joint. The lap joint specimens had been used in a fatigue test program by Carleton University and the National Research Council (NRC) of Canada [Scott, 1997; Eastaugh, et al., 1995]. Crack growth predictions for the specimens were performed as part of a program to develop an analytical corrosion damage assessment framework and the specimen test data were used to verify the predictions. The example is presented to demonstrate the risk analysis methodology.

The specimen, [Figure UD-4.1](#), is constructed of two 1 mm sheets of 2024-T3 clad aluminum with three rows of 4 mm 2117-T4 rivets (MS20426AD5-5). The rivet pattern has 25.4 mm pitch and row spacing with an edge margin of 9.1 mm. The test specimens were 25.4 cm wide with eight fasteners in each row across the width.

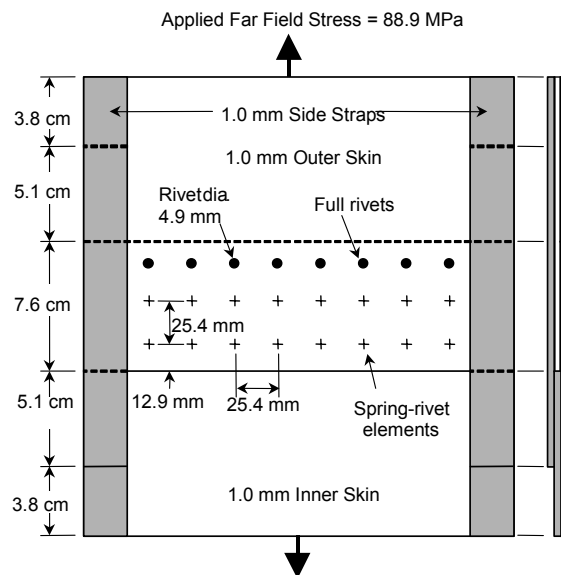


Figure UD-4.1. Schematic of Lap Joint Specimen.

Constant amplitude fatigue tests had been conducted at Carleton University on the lap joint specimens in non-corroded and corroded conditions with a constant amplitude far field stress of 88.9 MPa with $R = 0.2$. Details of the test procedure and resulting fatigue crack growth data are presented in Eastaugh, et al. [1995]. Nine non-corroded specimens were tested to failure to provide baseline data for comparison with corrosion specimens. Only data from these non-corroded baseline specimen tests are used in this example. Histories of crack size versus cycles for all cracks that initiated in the top row of rivet holes were recorded during the tests and were available for analysis. Examination of the histories showed that 95 percent or more of the joint life was expended when the lead crack reached about 9 mm and crack growth became unstable. Further, lead cracks initiated in accordance with two dominant scenarios. Scenario 1 is defined as a single crack originating from one side of a central hole. Scenario 2 is defined as approximately simultaneous, diametric cracks

originating from both sides of a central hole. Subsequent analysis showed significantly shorter lives for the double initial cracks. Analysis also showed that assuming both cracks were of equal size produced only 5 percent shorter lives than assuming one crack was twice the size of the second. Consequently, the assumptions were made that:

- a) joint life is determined by the initiation and growth of lead cracks that originate by one of two scenarios,
- b) cracks are of equal size in the double crack scenario, and,
- c) panel is essentially failed when the lead crack reaches 9 mm.

Because first cracks were simultaneously discovered in different holes in four of the nine data sets, there were a total of 13 lead cracks. Eight were from Scenario 1 and five were from Scenario 2. For this population of structural elements, it was assumed that probability of a randomly selected lap joint having a Scenario 1 lead crack was 8/13 and the probability of a randomly selected lap joint having a Scenario 2 lead crack was 5/13.

Crack growth analyses were performed for both scenarios [Trego, et al., 1998]. Stress analysis was performed using FRANC2D/L, a finite element, fracture mechanics analysis code with crack propagation capability [Wawryznek & Ingraffea, 1994; Swenson & James, 1997]. The resulting crack tip stress intensity factor values as a function of crack size were then input to the crack growth code AFGROW [Boyd, et al., 1998] for selected degrees of corrosion severity. The no-corrosion, constant amplitude peak stress of the baseline fatigue tests and crack growth analyses was 88.9 MPa with an R ratio of 0.2. Predicted cyclic life from 0.25 mm to 9 mm averaged about 30 percent more than the test data.

Corrosion severity was modeled in terms of percent thinning with the attendant increase in stress. To reflect corrosion severity, crack growth predictions were made for the somewhat arbitrarily selected levels of 0, 2, 5, 8, and 10 percent corrosive thinning by proportionate adjustments of the stress levels.

For the specimen conditions being modeled, the population of lap joint specimens has been divided into sub-populations based on combinations of two MSD scenarios and five corrosion severity levels. Cracking occurred in the two dominant MSD scenarios whose influence on crack growth was exhibited through the stress intensity factor. Corrosion severity was characterized by the metric of uniform thickness loss whose influence on crack growth is exhibited through the experienced stress levels. Each combination of MSD scenario and thickness loss produces a different crack growth analysis so that each combination must be individually analyzed in the risk analysis.

[Figure UD-4.2](#) illustrates the partitioning of the total population of the lap joints into the ten sub-populations. Every lap joint must fit into one of the sets of conditions defined by MSD scenario and thickness loss. The probability that cracks will initiate under Scenarios 1 and 2 are p_1 ($=8/13$) and p_2 ($=5/13$), respectively. The probability that a randomly selected lap joint will have uniform thickness loss level j is q_j . $POF(T/S_i, L_j) = POF_{ij}(T)$ is the probability of fracture as a function of time for the combination of MSD Scenario i and thickness loss j . The calculation of the unconditional probability of failure for a random lap joint in the fleet for each corrosion severity level is shown in the last column. An analogous calculation could be performed across severity levels to obtain composite failure probabilities for each MSD scenario.

Corrosion Severity	Proportion of Joints	Dominant MSD		Composite over MSD
		Scenario 1 p_1	Scenario 2 p_2	
Thickness Loss 1	q_1	$POF_{11}(T)$	$POF_{21}(T)$	$p_1POF_{11}(T)+p_2POF_{21}(T)$
Thickness Loss 2	q_2	$POF_{12}(T)$	$POF_{22}(T)$	$p_1POF_{12}(T)+p_2POF_{22}(T)$
Thickness Loss 3	q_3	$POF_{13}(T)$	$POF_{23}(T)$	$p_1POF_{13}(T)+p_2POF_{23}(T)$
Thickness Loss 4	q_4	$POF_{14}(T)$	$POF_{24}(T)$	$p_1POF_{14}(T)+p_2POF_{24}(T)$
Thickness Loss 5	q_5	$POF_{15}(T)$	$POF_{25}(T)$	$p_1POF_{15}(T)+p_2POF_{25}(T)$

$POF_{ij}(T) = POF(T/S_i, L_j) =$ Probability of failure for Scenario i , Thickness Loss j

$p =$ Proportion of lap joints with crack initiating under Scenario i

$q_j =$ Proportion of lap joints with uniform thickness loss at level j

Figure UD-4.2. Conditional Failure Probabilities for two MSD Scenarios and Five Levels of Uniform Thickness Loss.

An interpretation of the corrosion effects can be made directly from the PROF output. If an estimate of the distribution of thickness loss in the fleet is also available, the results of the individual runs of PROF can be combined using Equation (UD-4.1) to provide an overall fracture probability for a randomly-selected detail.

$$POF(T) = \sum POF(T/C_i) \cdot P(C_i) \quad (UD-4.1)$$

Further, the distribution of time to reach a fixed fracture probability can be inferred from the percentiles associated with the corrosion severity levels. These analyses will be demonstrated for corrosion in a representative lap joint.

It is realized that the risk analysis discussed herein does not account for the stress levels increasing as a result of increasing corrosion over the analysis period. At present, there are no accepted models for the corrosion damage growth (thickness loss) as a function of time so that the crack growth calculations are based on the state of corrosion at the beginning of the analysis interval. In reality, the stresses in the spectrum should be slowly increasing. If this effect could be accounted for in the deterministic analysis, the crack growth data input to PROF would reflect the change. However, the peak stress distribution would need to be made more severe at discrete increments. This added complexity could also be introduced by adding the additional level of conditioning and performing multiple PROF runs for each of the other ten conditions. This added level of conditioning provides insight into the total number of different runs that might be required to completely analyze a structure.

It might be noted that in the lap joint example of this paper, the peak stress distribution had no effect on the failure probability. The failure of the joint specimen was determined by reaching an unstable crack growth state when the lead crack reached 9 mm, a size far below the critical crack size for the applied far field stress.

PROF Input

The risk analysis for the lap joint corrosion example requires ten individual runs of PROF – two MSD scenarios and five stress levels for each of the MSD scenarios. The most significant inputs for the runs of this lap joint example are the crack growth projections and the initial crack size distribution. The other PROF inputs that reflect the changes between runs are the table of stress intensity factor divided by stress (K/σ) as a function of crack size and the distribution of peak stresses. These were changed between runs even though they had no effect on the results. K/σ came from the FRANC2D/L analysis. The peak stress distribution was estimated by a Gumbel extreme value distribution that had a mean at the appropriate constant amplitude level and a very small standard deviation to reflect the constant amplitude nature of the tests. Fracture toughness for the specimen was assumed to be normally distributed, with a mean and standard deviation of 152 and 11.4 $\text{Mpa}\sqrt{\text{m}}$, respectively. Because the example being modeled does not include inspection and repair cycles, reasonable, but arbitrary, data were used to define the inspection capability and the equivalent repair flaw size distributions.

The AFGROW crack growth curves for Scenarios 1 and 2 are presented in [Figures UD-4.3](#) and [UD-4.4](#), respectively. Each figure contains five crack growth curves reflecting the five levels of corrosion severity. The shorter crack growth lives from Scenario 2 are apparent from a comparison of these figures.

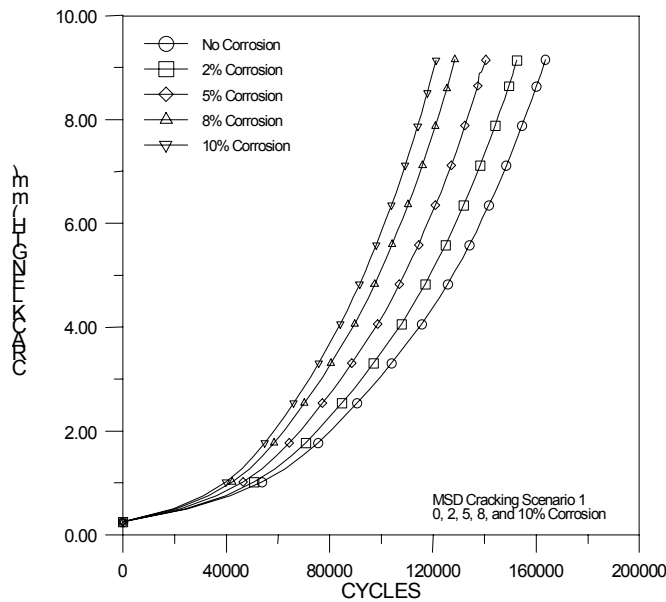


Figure UD-4.3. Crack Size versus Cycles for Scenario 1.

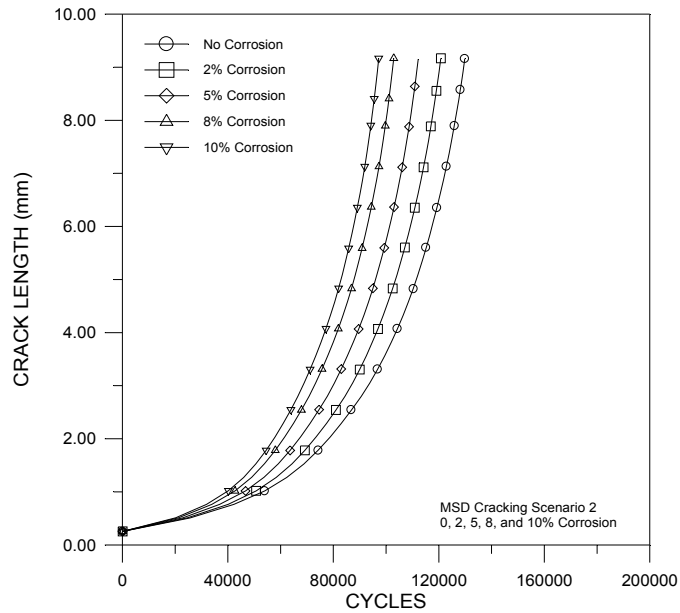


Figure UD-4.4. Crack Size versus Cycles for Scenario 2.

The initiating flaw size distribution was generated by back calculating from the sizes of the first observed lead cracks and their corresponding ages in the specimen test data. The back calculation was performed in two steps. First, the no-corrosion crack size versus cycles data of [Figures UD-4.3](#) and [UD-4.4](#) were used to determine the time at which each lead crack would have reached 0.25 mm. An exponential growth model was then fit to each lead crack to estimate an equivalent crack size at 50,000 cycles. Note that the inverse of this process returns each of the observed lead cracks to its original size and cycles.

The times to reach 0.25 mm for the cracks from the two MSD scenarios were statistically indistinguishable. Similarly, there was no statistical difference between the equivalent lead crack sizes from the two MSD scenarios at 50,000 cycles. The two sets of data were pooled to obtain the initiating flaw size distribution. The equivalent crack sizes at 50,000 cycles were fit with a mixture of two Weibulls as shown in [Figure UD-4.5](#). Also indicated in [Figure UD-4.5](#) are the MSD scenarios of origin of the lead cracks.

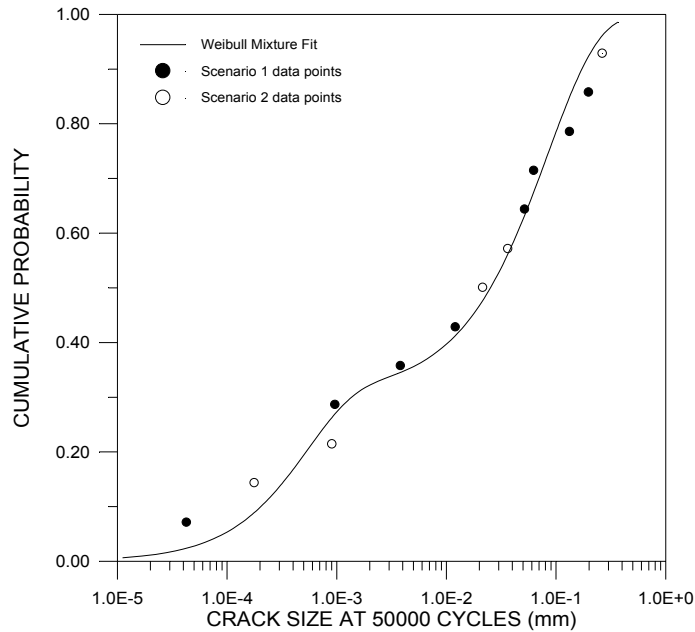


Figure UD-4.5. Weibull Mixture of Initial Crack Sizes.

PROF Risk Analysis Results

Probability of failure as a function of cycles was calculated for each of the ten combinations of cracking scenario and corrosion severity. Failure of the lap joint specimens was defined as the lead crack exceeding 9 mm, as previously discussed. [Figures UD-4.6](#) and [UD-4.7](#) present the failure probabilities as a function of experienced cycles for Scenarios 1 and 2, respectively. The failure probabilities behave as expected with increased risk of failure at a fixed age for Scenario 2 as compared to Scenario 1, and increasing risk of failure as the stress level increases due to corrosion material loss. These calculations do not account for any additional corrosive thinning after the start of the analysis.

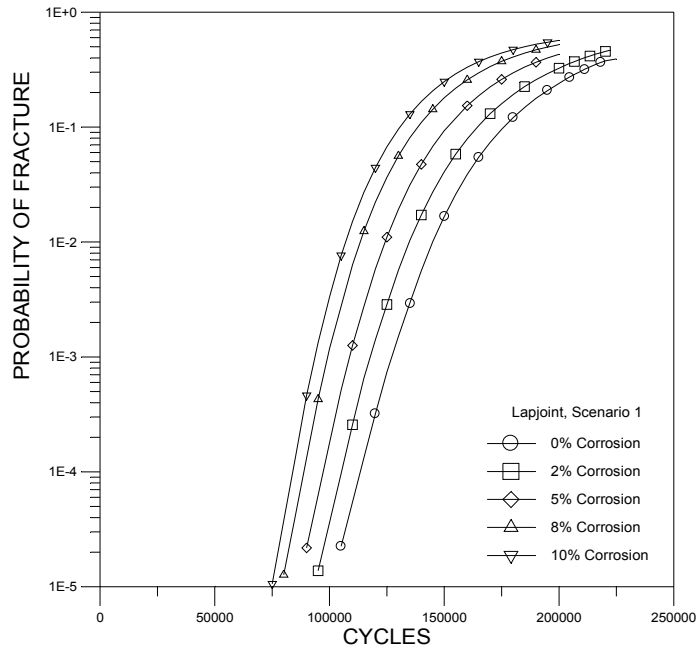


Figure UD-4.6. POF versus Cycles for Scenario 1.

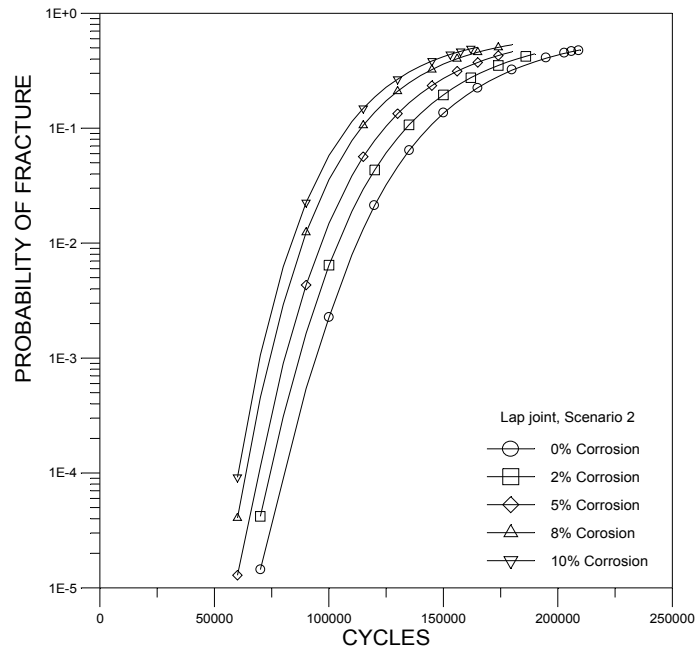


Figure UD-4.7. POF versus Cycles for Scenario 2.

As a gross check on the capability of the risk analysis methodology, [Figure UD-4.8](#) compares the calculated probability of failure as a function of cycles for 0% corrosion for Scenarios 1 and 2 to the observed distributions of failure times. Superimposed on the predicted failure probabilities are the observed cumulative distributions of the cycles to

failure from the lap joints that were the basis of the analysis. The observed cumulative distribution function was obtained by ordering the cycles to failure and dividing the ranks of the ordered times by the sample size plus one. That is,

$$F(T_i) = i/(n+1) \quad (\text{UD-4.2})$$

where i is the rank for T_i , the time at which the i^{th} crack exceeded 9 mm, and n is the number of observed cracks that met the definition for the scenario. Sample sizes for Scenarios 1 and 2 were eight and five, as noted earlier. The differences between the observed and predicted probabilities of failure are most likely due to the conservative deterministic life predictions or the extrapolation of the crack-size-versus-cycles relation that was required to obtain the initiating distribution of crack sizes.

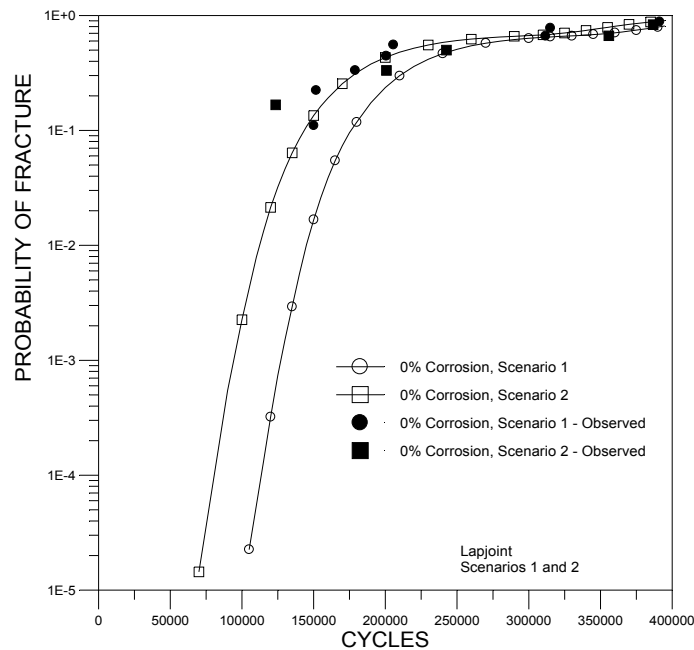


Figure UD-4.8. POF versus Cycles for Scenarios 1 and 2 Showing Comparison with Observed Data.

[Figures UD-4.6](#) and [UD-4.7](#) presented the conditional failure probabilities given the respective cracking scenario. The unconditional failure probability for a lap joint chosen at random from the population being analyzed is calculated as a weighted average of the conditional probabilities where the weighting factors are the proportion of specimens, which will initiate cracks in the two scenarios. See Equation UD-4.1 and [Figure UD-4.2](#). The weighting factors were estimated from the lap joint data in which eight of the 13 lead cracks were from Scenario 1 (initial lead crack from one side of the hole) and five of the 13 were from Scenario 2 (initial lead crack from diametrically opposite sides of the hole). Thus, $p_1 = 8/13$ and $p_2 = 5/13$. Using these factors, a comparison of the observed and predicted cycles to failure for the composite of the two scenarios without corrosion is

shown in [Figure UD-4.9](#). Again, the difference between the predicted and observed distributions of cycles to failure displays the somewhat non-conservative risks of the predicted failure probabilities.

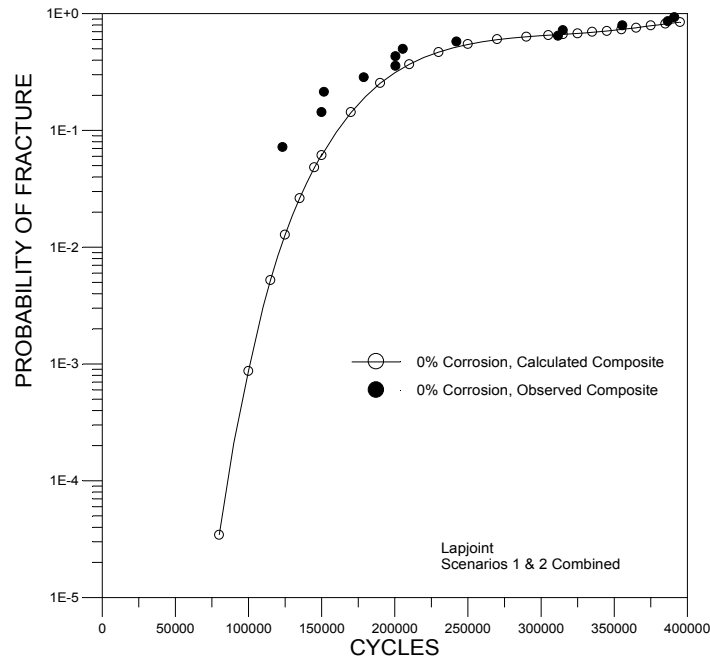


Figure UD-4.9. POF versus Cycles for Composite of Scenarios 1 and 2 Showing Comparison with Observed Data.

[Figure UD-4.10](#) summarizes the probabilities of failure for a randomly-selected lap joint that can have either MSD scenario and is subject to the expected stress history for five levels of corrosion severity. These results will be interpreted both in terms of the times to reach a defined probability of fracture (POF) and in terms of the relative differences in POF at a fixed number of cycles.

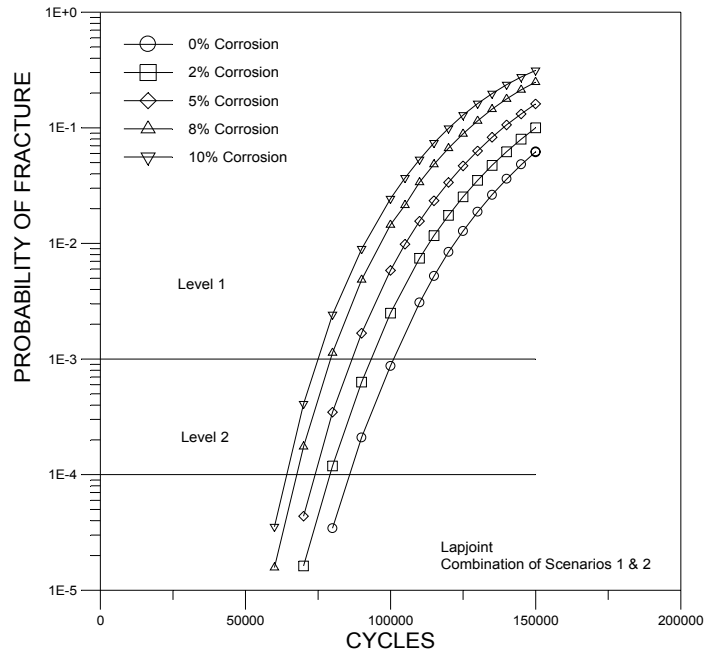


Figure UD-4.10. POF versus Cycles for Scenario Composites.

The cycles to reach a fixed POF for the different degrees of corrosion severity can be read from [Figure UD-4.10](#) as indicated, for example, at POF equal to 0.001 and 0.0001. Assume that the proportion of lap joints in the population that contain each of the five degrees of corrosion is known. Then the distribution of the time to reach the POF levels can also be inferred.

To illustrate, three representative distributions of corrosion damage were assumed, as given in [Table UD-4.1](#). Mix 1 is symmetric about a five percent material loss. Mix 2 is representative of a more severely corroded population. Mix 3 is representative of a less severely corroded population and is considered to be more representative of the corrosion that would be expected in aircraft.

Table UD-4.1. Assumed Distributions of Corrosion Damage.

Severity	Mix 1	Mix 2	Mix 3
0%	5	5	15
2%	25	15	40
5%	40	35	25
8%	25	35	15
10%	5	10	5

[Figure UD-4.11](#) presents a histogram of Mix 3. The corresponding percentage of lap joints would be expected to reach the selected POF level in the indicated number of cycles. The histogram for cycles to reach POF = 0.0001 for severity Mix 3 is shown in [Figure UD-4.12](#).

The cumulative distribution of time to reach the two POF levels for the three distributions of corrosion severity are shown in [Figure UD-4.13](#).

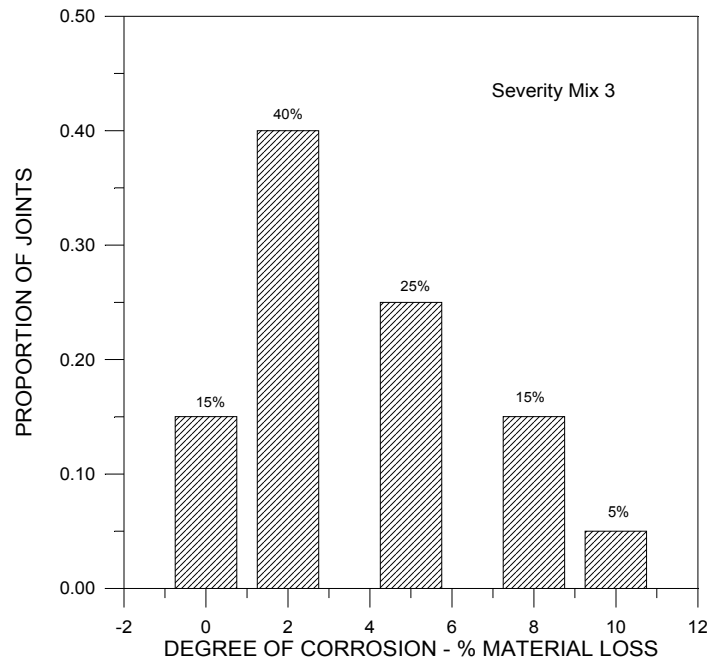


Figure UD-4.11. Example Histogram of Levels of Corrosion Damage – Severity Mix 3.

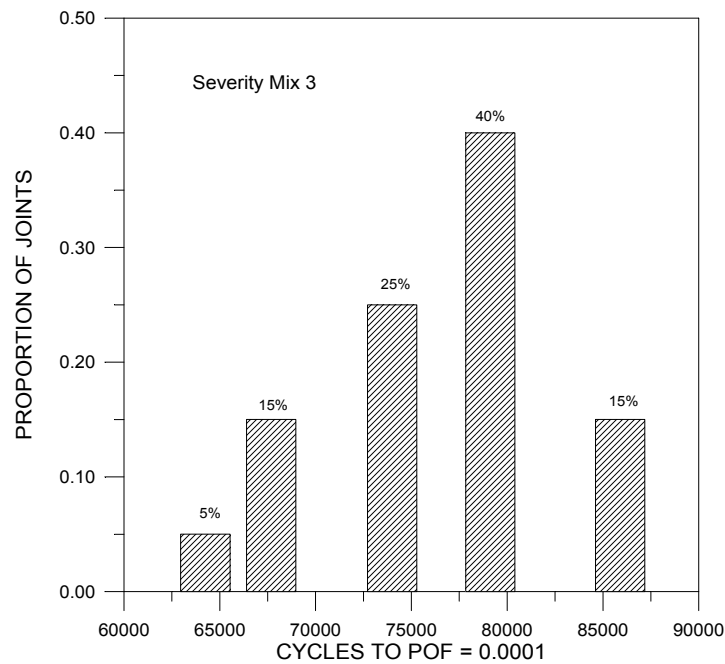


Figure UD-4.12. Example Histogram of Cycles to POF = 0.0001 – Severity Mix 3.

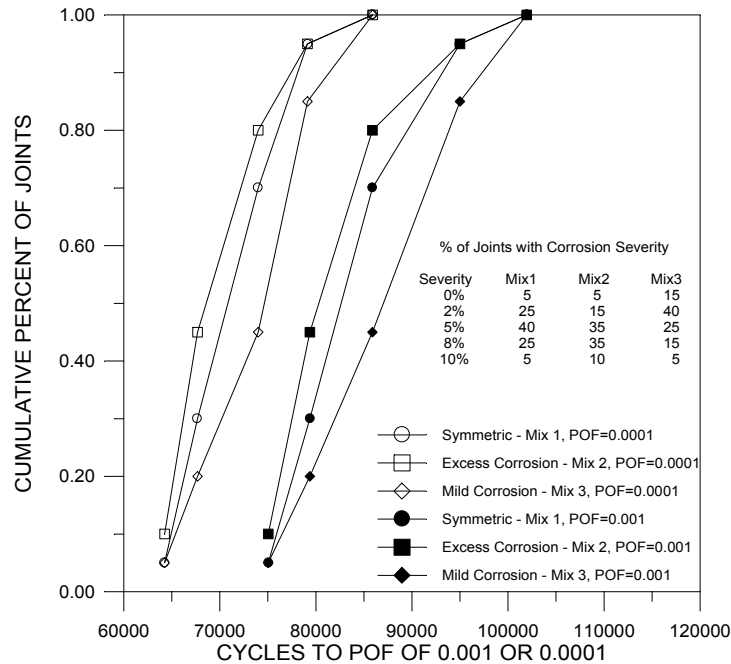


Figure UD-4.13. Cumulative Distribution of Cycles to Selected POF – 3 Corrosion Severities.

At a fixed number of cycles, the failure risk of a corroded lap joint can significantly exceed that of a non-corroded lap joint. To illustrate this difference, [Figure UD-4.14](#) presents the ratio of failure probabilities for each of the four degrees of corrosion severity to that of the non-corroded lap joints. The ratios are presented as a function of the failure probability of the non-corroded lap joint. The lap joint failure probability for the severity characterized by ten percent thinning can be 70 times greater than that of a non-corroded lap joint. If maintenance scheduling were based on keeping the failure probability below about 0.0001 to 0.001, a lap joint with ten percent corrosion thinning would have a 25 to 50 times greater chance of resulting in fracture.

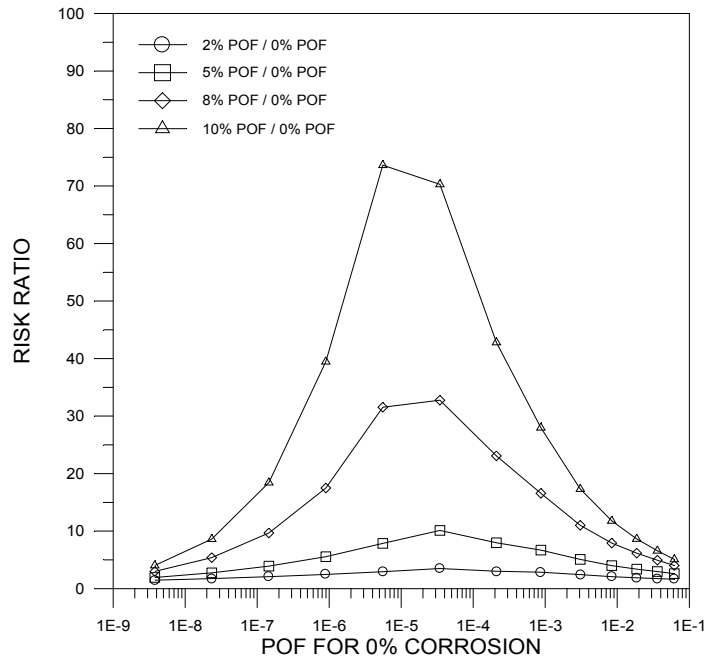


Figure UD4-14. Risk Ratios Normalized to No Corrosion Condition.

MSD/Corrosion Example Summary

This example demonstrates that it is possible to extend PROF to include probabilistic descriptions of the factors which influence fatigue life. In particular, a risk analysis was performed for fatigue failures in a representative lap joint in which the crack growth calculation was influenced by corrosion thickness loss and two scenarios of MSD. The basic approach to the analysis was to use deterministic crack growth calculations for different percentiles of the influencing factors in the probability of failure calculations, yielding conditional probabilities of failure. The full use of the analysis assumed that estimates of the proportion of Scenarios 1 and 2 and an estimate of the proportion of lapjoint with the discrete level of corrosive thinning were available, so that the conditional failure probabilities can be combined or otherwise interpreted.

In the lap joint example of this paper, the relative frequency of the two dominant MSD scenarios was estimated from data from a test program of the modeled specimen. Example distributions of thickness loss were assumed to demonstrate the calculations and interpretation. For this example, a ten percent thickness loss increased the failure probability by a factor of as much as 70 over the no-corrosion condition. Depending on the consequences of failure, inspection intervals based on the no-corrosion stress levels could pose a safety issue to corroded joints. The results were also used to demonstrate the generation of the distribution of time to a fixed risk.

References

Boyd, K., Harter, J.A., and Krishnan (1998), *AFGROW User's Manual Version 3.1.1*, WL-TR-97-3053, Air Force Research Laboratory, Wright-Patterson Air Force Base, Ohio.

Eastaugh, G.F., Simpson, D.L., Straznicky, P.V., and Wakeman, R.B. (1995), "A Special Uniaxial Coupon Test Specimen for the Simulation of Multiple Site Fatigue Crack Growth and Link-Up in Fuselage Skin Splices," National Research Council of Canada and Carleton University, AGARD-CP-568.

Scott, J.P. (1997), "Corrosion and Multiple Site Damage in Riveted Fuselage Lap Joints," Master's Thesis, Carleton University.

Swenson, D. and James, M. (1997) "FRANC2D/L: A Crack Propagation Simulator for Plane Layered Structures", Version 1.4 User's Guide, Kansas State University.

Trego, A., Cope, D., Johnson, P., and West, D. (1998) "Analytical Methodology for Assessing Corrosion and Fatigue in Fuselage Lap Joints," 1998 Air Force Corrosion Program Conference Proceedings, April 1998, Macon, Georgia.

Wawrzynek, P.A., and Ingraffea, A.R. (1994), "FRANC2D: A Two-Dimensional Crack Propagation Simulator, Version 2.7, User's Guide," NASA CR-4572.